NEW PHYSICS IN MOMENTUM-DEPENDENT WIDTHS AND PROPAGATORS

Wrishik Naskar
(based on 2501.08407, with C. Englert, M. Spannowsky)

9th Jul. 2025 — **EPS-HEP 2025**

Marseille, France

INTRODUCTION

- Collider observables depend on precise understanding particle widths, and propagators.

- The **Breit-Wigner** propagator (fixed width) (Nowakowski et al. 1993)

$$\boxed{i\,G(q^2) = \frac{i}{q^2 - m^2 + im\Gamma}}$$

- Collider observables depend on precise understanding particle widths, and propagators.

- The **Breit-Wigner** propagator (fixed width) (Nowakowski et al. 1993)

$$\boxed{i\,G(q^2) = \frac{i}{q^2 - m^2 + im\Gamma}}$$

- Propagators are susceptible to quantum corrections, q^2-dependent widths emerge from the **Dyson resummation** of 1PI insertions. (Denner 1993; Lehmann et al. 1955)

$i\,G(q^2) =$ 

- **Dyson-resummed** propagator: $G(q^2) = \frac{1}{q^2 - m^2 + \Sigma(q^2)}$.

INTRODUCTION

- Collider observables depend on precise understanding particle widths, and propagators.
- The **Breit-Wigner** propagator (fixed width) (Nowakowski et al. 1993)

$$\boxed{i\,G(q^2) = \frac{i}{q^2 - m^2 + im\Gamma}}$$

- Propagators are susceptible to quantum corrections, q^2-dependent widths emerge from the Dyson resummation of 1PI insertions. (Denner 1993; Lehmann et al. 1955)

$i\,G(q^2) =$ 

- Dyson-resummed propagator: $G(q^2) = \frac{1}{q^2 - m^2 + \Sigma(q^2)}$.
- **Running width:** $\Gamma(q^2) = \mathrm{Im}[\Sigma(q^2)]/m_{\mathrm{pole}} \Rightarrow$ Directly from the Optical Theorem.

(Cutkosky 1960; Newton 1976)

A SCALAR EXAMPLE: HIGGS

- The Higgs 2-point function:

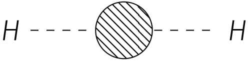

$$= -i(q^2 - m_H^2) - i\Sigma^H(q^2)$$

- The Dyson-resummed Higgs propagator:

$$i\, G_H(q^2) = \frac{i}{q^2 - m_H^2 + \Sigma_H(q^2)}$$

- The Higgs **running width**:

$$\boxed{\Gamma_H(q^2) = \frac{\mathrm{Im}\ \Sigma^H(q^2)}{m_H}} \quad \text{with} \quad \Gamma_H(q^2 = m_H^2) \approx 5.5\ \mathrm{MeV}$$

A SCALAR EXAMPLE: HIGGS

$$\boxed{\Gamma_H(q^2) = \frac{\text{Im}\,\Sigma^H(q^2)}{m_H}} \quad \text{with} \quad \Gamma_H(q^2 = m_H^2) \approx 5.5 \text{ MeV}$$

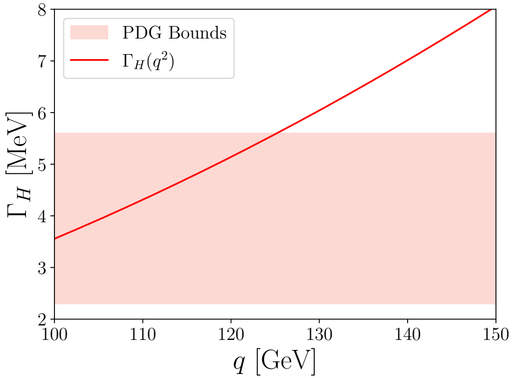

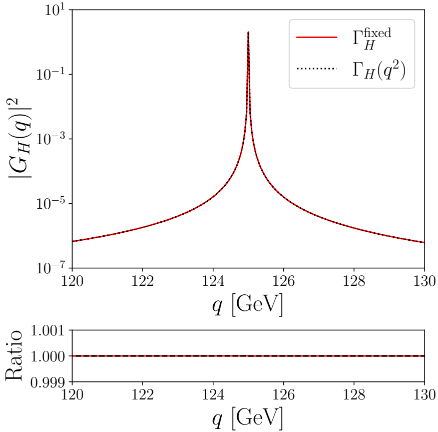

W BOSON

W_μ 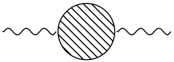 W_ν

$$= -ig_{\mu\nu}(q^2 - m_W^2) - i\left(g_{\mu\nu} - \frac{q_\mu q_\nu}{q^2}\right)\Sigma_T^W(q^2) - i\frac{q_\mu q_\nu}{q^2}\Sigma_L^W(q^2)$$

(Denner 1993)

- The **Dyson-resummed** W-propagator

$$iG_W^{\mu\nu}(q^2) = \frac{-i}{q^2 - m_W^2 + \Sigma_T^W(q^2)}\left(g^{\mu\nu} - \frac{q^\mu q^\nu}{q^2}\right).$$

- The **running** W**-width**

$$\boxed{\Gamma_W(q^2) = \frac{\mathrm{Im}\,\Sigma_T^W(q^2)}{m_W}} \quad \text{with} \quad \Gamma_W(q^2 = m_W^2) \approx 1.99\ \text{GeV}$$

W BOSON

$$\boxed{\Gamma_W(q^2) = \frac{\mathrm{Im}\ \Sigma_T^W(q^2)}{m_W}} \quad \text{with} \quad \Gamma_W(q^2 = m_W^2) \approx 1.99 \text{ GeV}$$

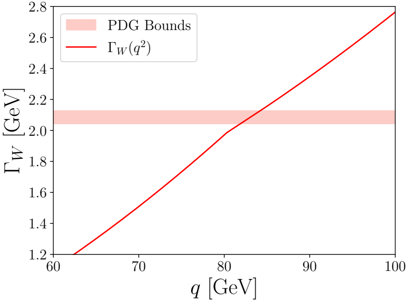

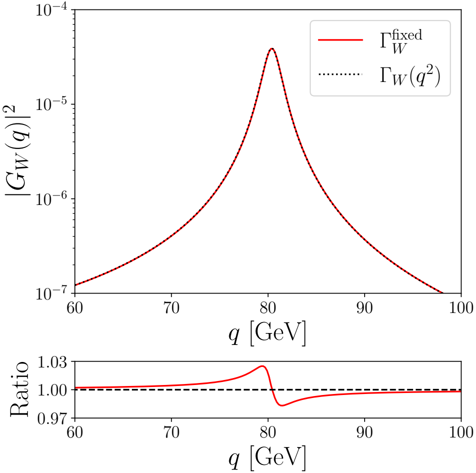

- *Impact on M_W measurements?*

- Several M_W measurements in the past few years, constraints from M_W^T.

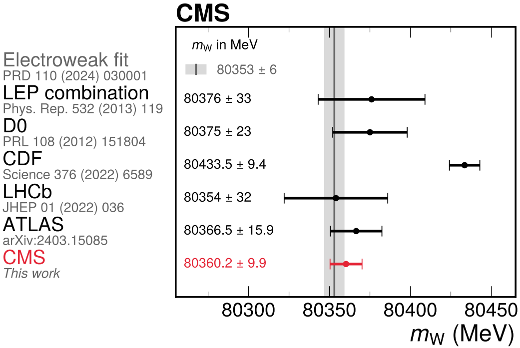

(CMS 2024)

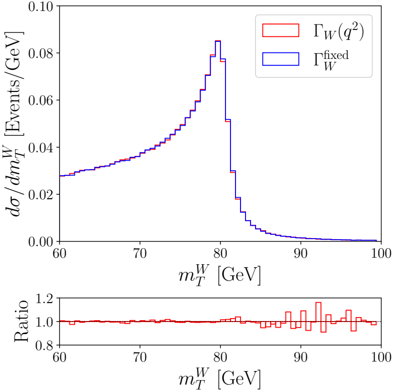

- *Percent level differences in $M_W^{inv.}$ lineshape difficult to resolve in M_W^T.*

THE TOP QUARK

t 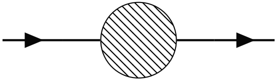 t $= i(\not{q} - m_t) + i\left[\not{q}\omega_- \Sigma_L^t(q^2) + \not{q}\omega_+\Sigma_R^t(q^2) + m_t\Sigma_S^t(q^2)\right]$

(Denner 1993)

- **Dyson-resummed** top propagator:

$$i\, G_t(q) = \frac{i}{\not{q}[1 + \omega_-\Sigma_L^t(q^2) + \omega_+\Sigma_R^t(q^2)] - m_t[1 - \Sigma_S^t(q^2)]}.$$

- For $\Gamma_t \ll m_t$, perturbatively, BW form (ref. backup for details)

$$i\, G_t(q) = i\frac{\not{q} + m_t}{q^2 - m_t^2 + im_t^2 \mathrm{Im}\left(\Sigma_L(q^2) + \Sigma_R(q^2) + 2\Sigma_S(q^2)\right)}.$$

(Dreiner et al. 2010)

THE TOP QUARK

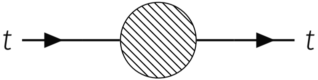

$$= i(\not{q} - m_t) + i\left[\not{q}\omega_- \,\Sigma_L^t(q^2) + \not{q}\omega_+\Sigma_R^t(q^2) + m_t\Sigma_S^t(q^2)\right]$$

(Denner 1993)

- Dyson-resummed top propagator ($\Gamma_t \ll m_t$):

$$i\,G_t(q) = i\frac{\not{q} + m_t}{q^2 - m_t^2 + i m_t^2 \mathrm{Im}\left(\Sigma_L(q^2) + \Sigma_R(q^2) + 2\Sigma_S(q^2)\right)}.$$

(Dreiner et al. 2010)

- **Running** top quark **width**

$$\boxed{\Gamma_t(q^2) = m_t\,\mathrm{Im}\left(\Sigma_L(q^2) + \Sigma_R(q^2) + 2\Sigma_S(q^2)\right)}, \qquad \Gamma_t(q^2 = m_t^2) \approx 1.44\ \mathrm{GeV}.$$

THE TOP QUARK

$$\boxed{\Gamma_t(q^2) = m_t \,\mathrm{Im}\left(\Sigma_L(q^2) + \Sigma_R(q^2) + 2\Sigma_S(q^2)\right)}, \qquad \Gamma_t(q^2 = m_t^2) \approx 1.44\ \text{GeV}.$$

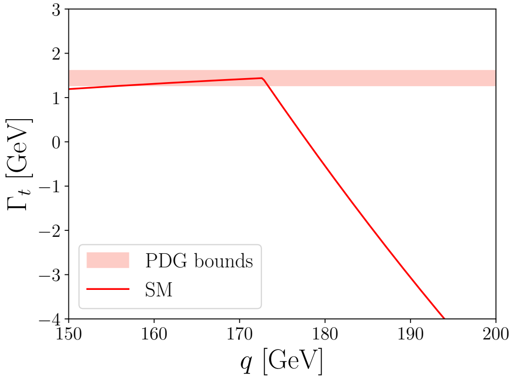

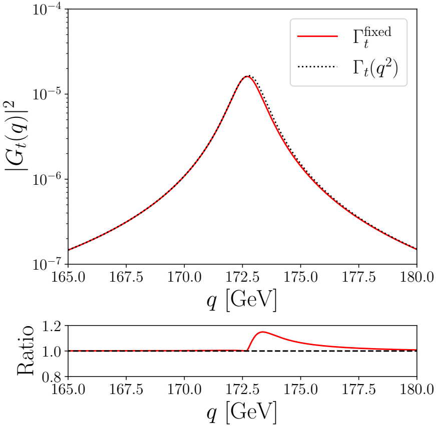

TOP 2 POINT AMPLITUDES

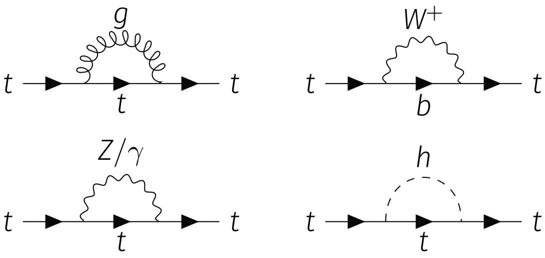

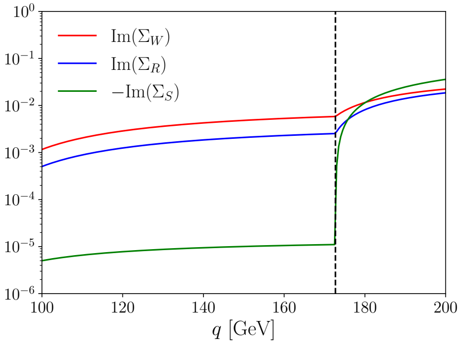

- Sharp increase Σ_S at $q^2 = m_t^2$ driven by the gluonic self-energy diagram.
- **New physics** affecting $\Sigma_{L,R,S}$ can lead to modifications to $m_t^{\text{inv.}}$
  $\Rightarrow$ Can be captured by precision measurements in the array of future colliders!

THE STANDARD MODEL EFT

- **SMEFT** provides an efficient way of capturing the effects of new UV physics.

$$\mathcal{L}_{\mathrm{SMEFT}} = \mathcal{L}_{\mathrm{SM}}^{d\leq 4} + \sum_{d>4} \sum_{i} \frac{C_i^{(d)}}{\Lambda^{d-4}} \mathcal{O}_i^{(d)}$$

(Brivio et al. 2019; Grzadkowski et al. 2010)

THE STANDARD MODEL EFT

- **SMEFT** provides an efficient way of capturing the effects of new UV physics.

$$\mathcal{L}_{\text{SMEFT}} = \mathcal{L}_{\text{SM}}^{d\leq 4} + \sum_{d>4} \sum_{i} \frac{C_i^{(d)}}{\Lambda^{d-4}} \mathcal{O}_i^{(d)}$$

(Brivio et al. 2019; Grzadkowski et al. 2010)

- Dimension-6 operators that can modify the top quark 2 point functions:

$\mathcal{O}_{tG}$	$(\bar{t}_L \sigma^{\mu\nu} T^A t_R)\tilde{\phi} G^A_{\mu\nu}$	$\mathcal{O}_{tW}$	$(\bar{t}_L \sigma^{\mu\nu} t_R)\tau^I \tilde{\phi} W^I_{\mu\nu}$
$\mathcal{O}_{t\phi}$	$(\phi^\dagger \phi)(\bar{t}_L t_R \phi)$	$\mathcal{O}_{tB}$	$(\bar{t}_L \sigma^{\mu\nu} t_R)\tilde{\phi} B_{\mu\nu}$

- $\mathcal{O}_{tG}, \mathcal{O}_{tB}, \mathcal{O}_{t\phi} \to$ high-p_T tails.
- $\mathcal{O}_{tW} \to$ Fixed Γ_t.

- Relatively weak constraints on these top-sector operators $\sim O(0.1 - 1)$ TeV^{-2}.

(Celada, Giani, et al. 2024; Garosi et al. 2023)

SMEFT EFFECTS IN Γ_t

$$C_{tX} = C_{tG} = C_{tW} = C_{tB} = C_{t\phi} = 1.5\ \text{TeV}^{-2}$$

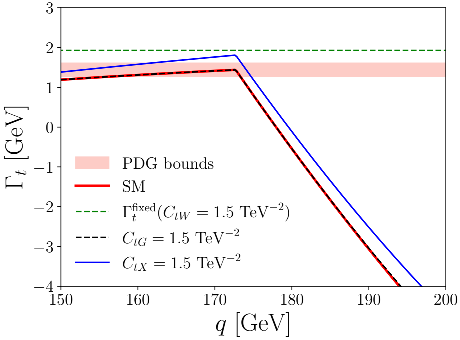

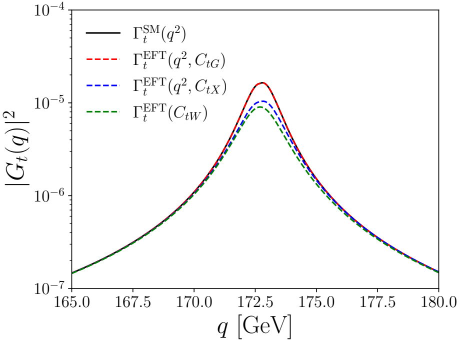

- Minor deviations in the high-p_T tails from $\mathcal{O}_{tG}$.
- Modified lineshapes can offer additional sensitivity to SMEFT coefficients.

LEPTON COLLIDERS

- Clean environment and low systematics $\rightarrow$ ideal for precision top physics .
- Accurate top lineshape reconstruction $\rightarrow$ can be sensitive to momentum-dependent width effects.

LEPTON COLLIDERS

- Clean environment and low systematics $\rightarrow$ ideal for precision top physics .
- Accurate top lineshape reconstruction $\rightarrow$ can be sensitive to momentum-dependent width effects.
- e^+e^- colliders (FCC-ee, ILC, CEPC, CLIC) probe $t\bar{t}$ via s-channel; FCC-ee is optimal near $t\bar{t}$ threshold, CLIC extends reach to 3 TeV (beamstrahlung-limited).

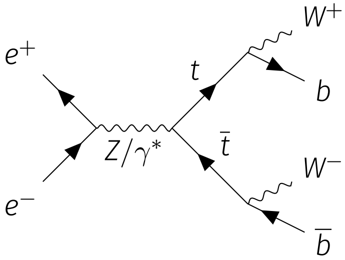

(Abada et al. 2019a; Abada et al. 2019b; Baer et al. 2013; CEPC 2018; Charles et al. 2018)

- Muon colliders also enable high-energy WBF top production $\rightarrow$ enhanced sensitivity to SMEFT-induced propagator distortions.

(Al Ali et al. 2022; Costantini et al. 2020; Celada, Han, et al. 2024)

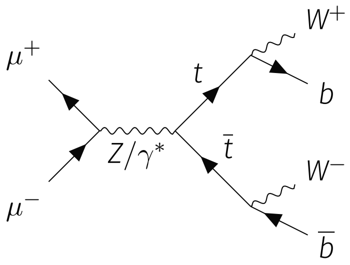

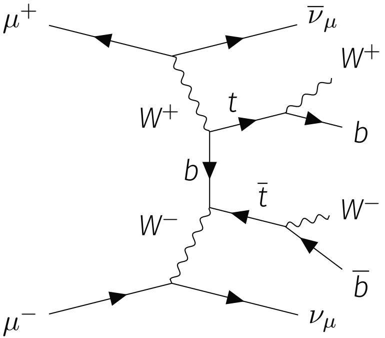

MUON COLLIDERS

- Muon colliders also enable high-energy WBF top production → enhanced sensitivity to SMEFT-induced propagator distortions.

(Al Ali et al. 2022; Costantini et al. 2020; Celada, Han, et al. 2024)

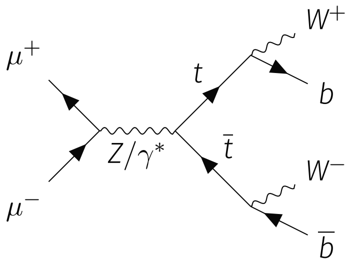

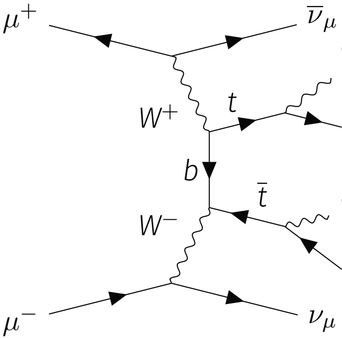

- Top lineshape reconstructed at $\sqrt{s} = 3, 10$ TeV using **semileptonic $t\bar{t}$ events** (propagator implementation on HELAS routines).

(Alwall et al. 2011; Murayama et al. 1992)

CONSTRAINTS FROM LINESHAPE

- Top lineshape reconstructed at $\sqrt{s} = 3, 10$ TeV using **semileptonic $t\bar{t}$ events.** 95% CL bounds on C_{tX} from a binned χ^2 statistic on the $m_t^{\text{inv.}}$.

$$\chi^2(C_{tX}) = (b^i_{\text{SM+EFT}}(C_{tX}) - b^i_{\text{SM}})V^{-1}_{ij}(b^j_{\text{SM+EFT}}(C_{tX}) - b^j_{\text{SM}}).$$

- Inverse covariance matrix contains relative uncertainties.

$$V_{ij} = b^i_{\text{SM}}\delta_{ij} + \epsilon_r b^i_{\text{SM}} b^j_{\text{SM}}.$$

$\mathcal{L}$	ϵ_r	$\sqrt{s} = 3$ TeV	$\sqrt{s} = 10$ TeV
5 ab^{-1}	25%	$(-0.83, 1.12)$ TeV^{-2}	$(-0.52, 0.48)$ TeV^{-2}
	10%	$(-0.54, 0.60)$ TeV^{-2}	$(-0.23, 0.21)$ TeV^{-2}
10 ab^{-1}	25%	$(-0.72, 0.91)$ TeV^{-2}	$(-0.42, 0.41)$ TeV^{-2}
	10%	$(-0.51, 0.57)$ TeV^{-2}	$(-0.20, 0.18)$ TeV^{-2}

CONSTRAINTS FROM LINESHAPE

- Top lineshape reconstructed at $\sqrt{s} = 3, 10$ TeV using **semileptonic $t\bar{t}$** events. 95% CL bounds on C_{tX} from a binned χ^2 statistic on the $m_t^{\text{inv.}}$.

$$\chi^2(C_{tX}) = (b^i_{\text{SM+EFT}}(C_{tX}) - b^i_{\text{SM}})V^{-1}_{ij}(b^j_{\text{SM+EFT}}(C_{tX}) - b^j_{\text{SM}}).$$

- Inverse covariance matrix contains relative uncertainties.

$$V_{ij} = b^i_{\text{SM}}\delta_{ij} + \epsilon_r b^i_{\text{SM}} b^j_{\text{SM}}.$$

$\mathcal{L}$	ϵ_r	$\sqrt{s} = 3$ TeV	$\sqrt{s} = 10$ TeV
5 ab^{-1}	25%	$(-0.83, 1.12)$ TeV^{-2}	$(-0.52, 0.48)$ TeV^{-2}
	10%	$(-0.54, 0.60)$ TeV^{-2}	$(-0.23, 0.21)$ TeV^{-2}
10 ab^{-1}	25%	$(-0.72, 0.91)$ TeV^{-2}	$(-0.42, 0.41)$ TeV^{-2}
	10%	$(-0.51, 0.57)$ TeV^{-2}	$(-0.20, 0.18)$ TeV^{-2}

- *How do these compare to bounds from SMEFT global fit methodologies?*

- C_{tG}, $C_{t\phi}$ are constrained in hadron colliders, C_{tW} and C_{tB} directly accessible at lepton colliders, analysed in detail in global fit literature.

(Celada, Giani, et al. 2024; Durieux et al. 2018; CLIC 2019; Buckley et al. 2016; Englert et al. 2017)

- Constraints from $\sigma^{\text{tot.}}$, A_{FB} adapted for muon colliders offer significantly stronger bounds.

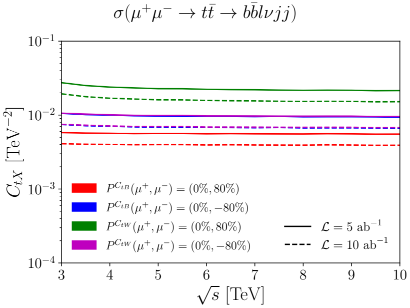

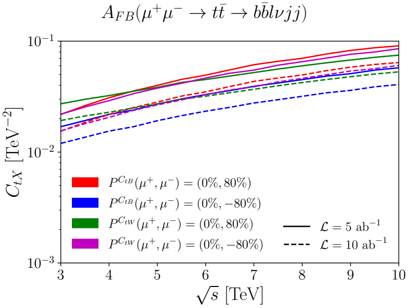

CONCLUSIONS AND OUTLOOK

- Momentum-dependent widths are relevant pseudo-observables for future precision physics.
- Effects are **small** for Higgs, W-boson, but the **top quark running width** shows **significant deviations** in invariant mass lineshape, above m_t threshold.

CONCLUSIONS AND OUTLOOK

- Momentum-dependent widths are relevant pseudo-observables for future precision physics.
- Effects are **small** for Higgs, W-boson, but the **top quark running width** shows **significant deviations** in invariant mass lineshape, above m_t threshold.
- SMEFT parameterisation offers a novel handle on BSM physics, altering the invariant mass lineshape.
- **Future muon colliders** enable precise measurements of **top quark lineshapes**, SMEFT-induced deviations in the running width can be probed beyond current hadron collider sensitivity.
- Global fits indeed perform slightly better, however incorporating finite width into analyses is **important** for precision physics.

THANK YOU

BACKUP SLIDES

ON-SHELL RENORMALISATION CONDITIONS

- Higgs, W boson

$$\mathrm{Re}\ \Sigma^{H,W}(q^2)\big|_{q^2=m_H^2,m_W^2} = \mathrm{Re}\ \frac{\partial \Sigma^{H,W}(q^2)}{\partial q^2}\bigg|_{q^2=m_H^2,m_W^2} = 0.$$

- Top quark

$$\begin{aligned}
&\mathrm{Re}\ \Sigma_L^t(q^2)\big|_{q^2=m_t^2} + \mathrm{Re}\ \Sigma_S^t(q^2)\big|_{q^2=m_t^2} = 0,\\
&\mathrm{Re}\ \Sigma_R^t(q^2)\big|_{q^2=m_t^2} + \mathrm{Re}\ \Sigma_S^t(q^2)\big|_{q^2=m_t^2} = 0,\\
&\mathrm{Re}\ \Sigma_L^t(q^2)\big|_{q^2=m_t^2} + \mathrm{Re}\ \Sigma_R^t(q^2)\big|_{q^2=m_t^2}\\
&\qquad +2m_t^2 \frac{\partial}{\partial q^2}\left[\mathrm{Re}\ \Sigma_L^t(q^2) + \mathrm{Re}\ \Sigma_R^t(q^2) + 2\mathrm{Re}\ \Sigma_S^t(q^2)\right]\big|_{q^2=m_t^2} = 0
\end{aligned}$$

(Denner 1993)

EXAMPLE DYSON RESUMMATION: TOP QUARK

$$iG(\not{q}, q^2) =$$

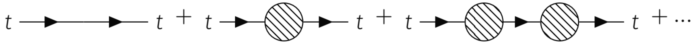

$$= \frac{i}{\not{q} - m_t} + \left[\frac{i}{\not{q} - m_t} i\Sigma_2^t(\not{q}, q^2) \frac{i}{\not{q} - m_t}\right] + \left[\frac{i}{\not{q} - m_t} i\Sigma_2^t(\not{q}, q^2) \frac{i}{\not{q} - m_t} i\Sigma_2^t(\not{q}, q^2) \frac{i}{\not{q} - m_t}\right] + \ldots$$

$$= \frac{i}{\not{q} - m_t}\left[1 - \left(\frac{\Sigma_2^t(\not{q}, q^2)}{\not{q} - m_t}\right) + \left(\frac{\Sigma_2^t(\not{q}, q^2)}{\not{q} - m_t}\right)^2 - \ldots\right]$$

$$= \frac{i}{\not{q} - m_t}\left(\frac{1}{1 + \frac{\Sigma_2^t(\not{q}, q^2)}{\not{q} - m_t}}\right)$$

$$= \frac{i}{\not{q} - m_t + \Sigma_2^t(\not{q}, q^2)}$$

$$\boxed{\Sigma_2^t(\not{q}, q^2) = \not{q}\omega_- \Sigma_L^t(q^2) + \not{q}\omega_+ \Sigma_R^t(q^2) + m_t \Sigma_S^t(q^2)}$$

TOP RUNNING WIDTH

The full expression for the top quark propagator:

$$i\,G(q) = \frac{i}{\not{q}[1+\omega_-\Sigma_L^t(q^2)+\omega_+\Sigma_R^t(q^2)] - m_t[1-\Sigma_S^t(q^2)]}.$$

The Breit-Wigner form:

$$iG(q) = i\frac{\not{q}[1+\omega_-\Sigma_L^t(q^2)+\omega_+\Sigma_R^t(q^2)] + m_t[1-\Sigma_S^t(q^2)]}{q^2[1+\Sigma_L^t(q^2)][1+\Sigma_R^t(q^2)] - m_t^2[1-\Sigma_S^t(q^2)]^2}.$$

Isolating the q^2 term in the denominator,

$$iG(q) = i\frac{\not{q}[1+\omega_-\Sigma_L^t(q^2)+\omega_+\Sigma_R^t(q^2)] + m_t[1-\Sigma_S^t(q^2)]}{(1+\Sigma_L^t(q^2))(1+\Sigma_R^t(q^2))\left(q^2 - \frac{m_t^2[1-\Sigma_S^t(q^2)]^2}{[1+\Sigma_L^t(q^2)][1+\Sigma_R^t(q^2)]}\right)},$$

(Dreiner et al. 2010)

TOP RUNNING WIDTH

$$iG(q) = i\frac{\not{q}[1+\omega_-\Sigma_L^t(q^2)+\omega_+\Sigma_R^t(q^2)]+m_t[1-\Sigma_S^t(q^2)]}{(1+\Sigma_L^t(q^2))(1+\Sigma_R^t(q^2))\left(q^2-\frac{m_t^2[1-\Sigma_S^t(q^2)]^2}{[1+\Sigma_L^t(q^2)][1+\Sigma_R^t(q^2)]}\right)}.$$

The pole can be identified as

$$M_{t,\mathrm{pole}}^2 - iM_{t,\mathrm{pole}}\Gamma_t = \left.\frac{m_t^2(1-\Sigma_S)^2}{(1+\Sigma_L)(1+\Sigma_R)}\right|_{q^2=m_t^2}.$$

To one-loop order, perturbatively, $m_t = 172.7$ GeV,

$$M_{t,\mathrm{pole}}^2 - iM_{t,\mathrm{pole}}\Gamma_t = m_t^2\left(1-\Sigma_L-\Sigma_R-2\Sigma_S\right)\Big|_{q^2=m_t^2}.$$

$$M_{t,\mathrm{pole}} = m_t\left.\left(1-\frac{1}{2}\Sigma_L-\frac{1}{2}\Sigma_R-\Sigma_S\right)\right|_{q^2=m_t^2} \approx 172.7\ \mathrm{GeV}$$

$$\Gamma_t(q^2) = m_t\,\mathrm{Im}\left(\Sigma_L+\Sigma_R+2\Sigma_S\right), \quad \Gamma_t(q^2=m_t^2)\approx 1.44\ \mathrm{GeV}.$$

(Dreiner et al. 2010)

- Γ_t measured at 13 TeV collisions via template fit to M_{lb} in dileptonic $t\bar{t}$.

(ATLAS 2019)

$\Rightarrow$ M_{lb}: inv. mass of final state lepton and associated b-jet.

- Mildly sensitive to Γ_t, shifts from q^2 effects at the few-percent level.
- Overall sensitivity to q^2-dependent effects is low $\Rightarrow$ **limited** BSM reach at the (HL-)LHC.

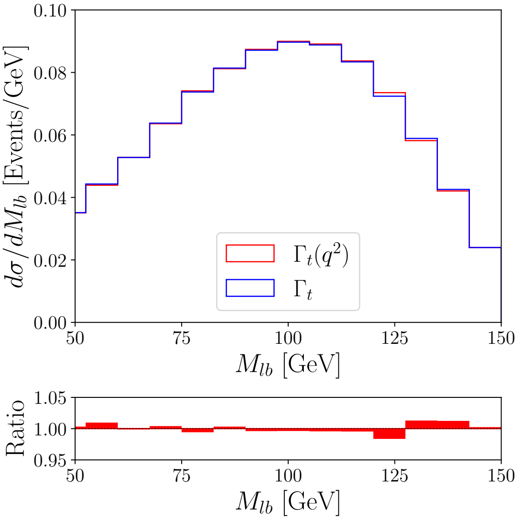

GLOBAL FIT CONSTRAINTS

- Current Constraints in the top sector:

Coefficient	Individual $\mathcal{O}(\Lambda^{-2})$	Marginalised $\mathcal{O}(\Lambda^{-2})$	Individual $\mathcal{O}(\Lambda^{-4})$	Marginalised $\mathcal{O}(\Lambda^{-4})$
$C_{t\phi}$	[-1.199, 0.327]	[-4.142, 2.831]	[-1.168, 0.333]	[-3.035, 3.527]
C_{tW}	[-0.087, 0.029]	[-0.180, 0.147]	[-0.082, 0.029]	[-0.177, 0.141]
C_{tZ}	[-0.034, 0.102]	[-4.999, 12.276]	[-0.038, 0.094]	[-0.645, 1.027]
C_{tG}	[0.004, 0.084]	[-0.050, 0.199]	[0.003, 0.080]	[0.019, 0.180]

- Upper bounds at HL-LHC + FCC-ee:

Coefficient	Individual $\mathcal{O}(\Lambda^{-2})$	Marginalised $\mathcal{O}(\Lambda^{-2})$	Individual $\mathcal{O}(\Lambda^{-4})$	Marginalised $\mathcal{O}(\Lambda^{-4})$
$C_{t\phi}$	2.96×10^{-1}	2.18	2.88×10^{-1}	2.19
C_{tW}	3.83×10^{-3}	5.82×10^{-2}	3.74×10^{-3}	6.02×10^{-2}
C_{tZ}	4.79×10^{-3}	6.92×10^{-2}	4.70×10^{-3}	7.19×10^{-2}
C_{tG}	2.38×10^{-2}	6.89×10^{-2}	2.45×10^{-2}	6.52×10^{-2}

(Celada, Giani, et al. 2024)

SENSITIVITY CALCULATIONS FROM σ AND A_{FB}

- Process: $\mu^+\mu^- \to t\bar{t}$.
- Total cross-section (σ) and forward-backward asymmetry (A_{FB}) are sensitive to EFT operators:

$$A_{\mathrm{FB}} = \frac{\sigma_{\mathrm{FB}}}{\sigma}, \quad \sigma_{\mathrm{FB}} = \int_{-1}^{1} d\cos\theta_t \,\mathrm{sign}(\cos\theta_t)\, \frac{d\sigma}{d\cos\theta_t}$$

- EFT observable expansion and sensitivity:

$$o = o_{\mathrm{SM}} + C_i o_i + C_i C_j o_{ij} + \ldots, \quad S_i^o = \frac{1}{o}\frac{\partial o}{\partial C_i}\bigg|_{C_i=0} = \frac{o_i}{o_{\mathrm{SM}}}$$

- 95% CL bounds from σ and A_{FB} are stronger than from lineshape fits.

(Durieux et al. 2018; CLIC 2019)

TOPFITTER CONSTRAINTS FOR MUON COLLIDERS

- Process: $\mu^+\mu^- \to t\bar{t}$.
- χ^2 distribution to determine the constraints on the Wilson coefficients.

$$\chi^2(C_{tX}) = \frac{(\sigma[C_{tX}] - \sigma)^2}{\sigma}$$

$\Rightarrow$ $\sigma = \sigma_{SM}(1 + \Sigma)$, σ_{SM}: SM cross-section.

$\Rightarrow$ Σ: Uncertainties on the cross-section

$\mathcal{L}$	Wilson coefficient	$\sqrt{s} = 3$ TeV	$\sqrt{s} = 10$ TeV
5 ab^{-1}	C_{tB}	$(-0.02, 0.15)$ TeV^{-2}	$(-0.02, 0.04)$ TeV^{-2}
	C_{tW}	$(-0.02, 0.24)$ TeV^{-2}	$(-0.03, 0.05)$ TeV^{-2}
10 ab^{-1}	C_{tB}	$(-0.02, 0.14)$ TeV^{-2}	$(-0.02, 0.03)$ TeV^{-2}
	C_{tW}	$(-0.02, 0.23)$ TeV^{-2}	$(-0.02, 0.05)$ TeV^{-2}

(Buckley et al. 2016)